

# Modeling a Two-Stage High-Power Bismuth Anode Layer Thruster and its Plume

IEPC-2005-045

*Presented at the 29<sup>th</sup> International Electric Propulsion Conference, Princeton University,  
October 31 – November 4, 2005*

Michael Keidar<sup>\*</sup>, and Yongjun Choi<sup>†</sup> and Iain D. Boyd<sup>‡</sup>  
*University of Michigan, Ann Arbor MI*

**Abstract:** A model of a two-stage thruster with anode layer is developed based on a two-dimensional hydrodynamic approach. Each stage is considered separately, while the solution of the 1<sup>st</sup> stage provides the boundary conditions for the 2<sup>nd</sup> stage. Current-voltage characteristic of the discharge in the 1<sup>st</sup> stage is calculated and is found to be in agreement with experiment. In the acceleration channel the plasma-wall interactions are studied and expansion of the high voltage sheath near the acceleration channel wall is investigated. It is predicted that under the typical conditions the sheath expands significantly and the quasi-neutral plasma region is confined in the middle of the channel. For instance, in the case of a 3 kV discharge voltage, the sheath thickness is about 1 cm, which is a significant portion of the channel width. It is shown that near-wall sheath expansion leads to a shorter acceleration region. Wall erosion by the energetic ions is calculated. The erosion profiles and the total erosion rate generally agree well with available experimental data. Plasma flow analysis provides the boundary conditions for the plume expansion study. The plume model is partially validated by comparison of the ion current density distribution with experimental data.

## Nomenclature

$\beta$	= ionization rate
$\nu_{ef}$	= effective electron collision frequency
$\nu_w$	= frequency of electron collisions with walls
$\Delta\phi_w$	= voltage drop across the sheath near the channel wall
$A$	= cross section
$Q_j$	= Joule heat
$E_z$	= axial component of the electric field
$j_e$	= electron current density
$j_e^{\text{th}}$	= electron thermal current density
$j_d$	= discharge current density
$Q_w$	= electron energy losses to the walls
$n$	= plasma density
$n_a$	= neutral density
$V$	= velocity
$V_s$	= ion velocity at the sheath edge,

---

<sup>\*</sup> Research Scientist, Department of Aerospace Engineering, keidar@umich.edu.

<sup>†</sup> Graduate Student, Department of Aerospace Engineering.

<sup>‡</sup> Professor, Department of Aerospace Engineering.

$U$  = voltage across the sheath,  
 $s$  = sheath thickness,  
 $\varepsilon$  = permittivity of vacuum,  
 $N_s$  = plasma density at the sheath edge,  
 $m_i$  = ion mass  
 $Q_{ion}$  = ionization energy losses  
 $U_i$  = ionization potential  
 $i, a, e$  = subscript for ions, neutral atoms and electrons, respectively

## I. Introduction

**A**MONG Hall thruster technologies, the thruster with anode layer (TAL) seems to have the widest technical capabilities. Nowadays Hall thrusters in general are among the most advanced and efficient types of electrostatic propulsion devices. The electric field in the Hall thruster is perpendicular to the magnetic field and thus passing the electron current across a magnetic field leads to an electron closed drift or Hall drift, that provides the necessary gas ionization. In the Hall thruster the particle acceleration takes place in a quasi-neutral plasma and thus is not limited by space charge effects unlike the ion thruster counterpart. Since the time of the original idea introduction in the mid 1960's (see Refs. 1,2,3,4,5,6,7) numerous experimental and theoretical investigations have been conducted.<sup>8,9</sup>

In a TAL, the ion acceleration takes place over a thin layer with length of about the electron Larmor radius. This is why the term "anode layer" was attributed to the Hall thruster with metal walls.<sup>1</sup> In this thruster, an electric discharge in the ExB fields is created in the gap between magnetic poles where closed electron drift takes place. In this magnetized layer, the neutral atoms are ionized and accelerated. In some cases, a substantial fraction of the ions is directed toward the wall that limits the discharge in the radial direction and protects the magnetic poles from erosion. Ion interaction with walls leads to wear of these walls due to ion bombardment and results in a shortened lifetime of such accelerators.

Recently an interest in development of high power Hall thrusters was renewed due to the fact that TAL technology has wide technical capabilities and range of parameters.<sup>10,11,12</sup> In particular, since reduced erosion of various thruster components, such as electrodes, insulators, screens, etc. is critical for the long term operation of the thruster, the TAL variant of Hall thruster technology seems to be beneficial since it has a very small acceleration region and therefore small area in contact with ions of materials where possible erosion occurs. Recently, a two-stage TAL that was developed more than 25 years ago by TsNIIMASH was presented.<sup>11</sup> This thruster using bismuth as the propellant demonstrated increasing efficiency with operating voltage through 8 kV and specific impulse in the range of 2000-5000s at power levels of 10-34 kW. Having many advantages, bismuth was found to be a suitable option as

a propellant. Bismuth has low ionization potential, is heavy and significantly less toxic than mercury, while much cheaper than xenon<sup>11</sup>.

It was demonstrated that TALs can operate in both single and two stage regimes; in the two-stage regime, ionization and acceleration take place in two separate discharges, so that at the exit plane of the first stage, the plasma is highly ionized and additional ionization in the second stage is insignificant.<sup>11</sup> It was demonstrated that the two-stage regime of operation has many advantages, for instance the possibility to achieve much higher specific impulse.<sup>13</sup> When a two-stage thruster is considered, the most important region in terms of long time operation is the second acceleration stage in which a very large voltage drop is applied. While, theoretically, discharges in both stages are separate, there is a coupling in which the second stage discharge affects the first stage discharge. Below some low discharge voltage at the first stage limit, which is about 250 V, the discharge in the first stage cannot be sustained without the second stage.<sup>14</sup> In this mode the discharge is diffuse and it was found that plume divergence is minimal.<sup>14</sup> Thus, this discharge mode is preferable for a two-stage thruster.

Recently it was shown that an important aspect of high power TAL's is the sheath formation near the channel wall.<sup>15</sup> Typically in a TAL, the channel walls have potential, which is equal to the cathode potential, leading to a significant potential drop between the wall and the plasma. As a result, a high-voltage space charge sheath is formed and the sheath thickness can be comparable to the channel width. Therefore, a transition between quasi-neutral and space charge regimes can occur in the case of a high voltage in the second stage.<sup>15</sup> This transition can have a significant effect on the TAL operation and therefore is extremely important for practical applications.

In this paper various aspects of the two-stage high power bismuth TAL are studied. Models of plasma flow in the 1<sup>st</sup> and 2<sup>nd</sup> stages are developed based on a 2D hydrodynamic approach. In the 2<sup>nd</sup> stage, plasma-wall interactions are studied in detail. In particular, erosion of the channel wall due to energetic ion impact is analyzed. Plasma flow analysis in the thruster provides boundary conditions for the plume simulation. Plasma plume expansion under various conditions is investigated. The overall model is validated by comparison with existing experimental data.

## **II. The Model of TAL Plasma Flow**

The considered thruster has a two-stage configuration in order to separate the ion production and acceleration zones. Previously, a model of the 2<sup>nd</sup> acceleration stage was developed<sup>15</sup>. Recent efforts are concentrated on development of the 1<sup>st</sup> ionization stage. To this end, a 2D hydrodynamic model of the 1<sup>st</sup> stage of the VHITAL-160 is developed. The diffuse form of the discharge in the 1<sup>st</sup> stage is studied. This form of the discharge is sustained by the acceleration stage according to previous experiments. Therefore the model of the 1<sup>st</sup> stage is coupled with the acceleration stage [15] and initially electron temperature is used as a downstream boundary condition.

In this section, we consider the plasma flow, which starts at the anode of the 1<sup>st</sup> stage. Quasi-neutrality is assumed and therefore the plasma presheath-sheath interface is considered as the lateral boundary for the plasma flow region. This model was described in detail elsewhere.<sup>16</sup> Here we just briefly review the main points of the model. We employ a hydrodynamic model in a 2D domain assuming that the system reaches a steady state as shown in Fig.1. A radial component of the magnetic field only is considered. The momentum and mass conservation equations for electrons, ions and neutrals under such conditions have the following form:

$$nm_i(\mathbf{V}_i \cdot \nabla) \mathbf{V}_i = ne\mathbf{E} - \nabla P_i - \beta nm_i n_a (\mathbf{V}_i - \mathbf{V}_a) \quad (1)$$

$$\nabla \cdot (\mathbf{V}_i n) = \beta n n_a \quad (2)$$

$$\nabla \cdot (\mathbf{V}_a n_a) = -\beta n n_a \quad (3)$$

$$0 = -en(\mathbf{E} + \mathbf{V}_e \times \mathbf{B}) - \nabla P_e - n \nu_{ef} m_e (\mathbf{V}_e - \mathbf{V}_i) \quad (4)$$

$$\frac{3}{2} \partial (j_e T_e) / \partial z = Q_j - Q_w - Q_{ion} \quad (5)$$

where  $Q_j = j_e E$  is the Joule heat,  $Q_w = \nu_w n (2eT_e + e\Delta\phi_w)$  represents the electron energy losses to the walls, and  $Q_{ion} = en_a n U_i \beta$  represents ionization energy losses. The ionization rate is taken from Ref. 17. To simplify the problem without missing the major physical effects, we consider one-dimensional flow of the neutrals, i.e.  $V_a = V_{az}$ . Finally, electron transport is considered in a one-dimensional framework along the channel median. Since only the radial magnetic field component is considered, the electron transport is much greater in the azimuthal direction ( $\mathbf{E} \times \mathbf{B}$  drift) than in the axial direction (drift diffusion due to collisions). We consider that electron transport across the magnetic field is due to several collision mechanisms: electron-neutral collisions and anomalous (Bohm) diffusion:  $\nu_{ef} = \nu_{en} + \nu_B$  where  $\nu_{ef}$  is the effective electron collision frequency.

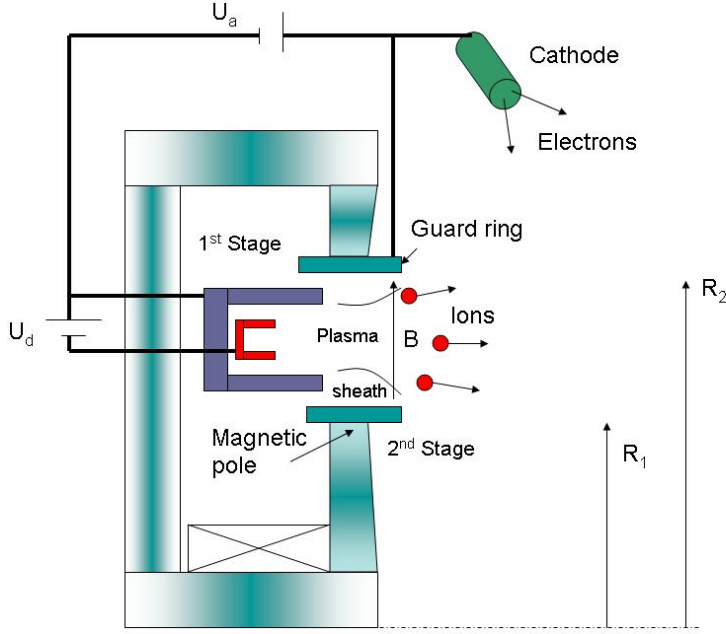


**Fig.1. Schematics of the thruster and computational domain**

The model includes Bismuth evaporation and current continuity analysis at the anode. The near anode sheath is considered for which the potential drop is

$$\Delta\varphi_a = \ln\left(\frac{j_d + enC_s}{j_e^{th}}\right) \quad (6)$$

The discharge current in the range of 4-6 A is considered. It is found that bismuth ionization is very efficient and occurs in the vicinity of the evaporated Bi surface. Current-voltage characteristic of the first stage is calculated and is found to be in a good agreement with experiment as will be described in the next section.

### III. Analysis of the ionization stage in a two-stage TAL

In this section, we describe results of computation of the plasma flow and electric characteristics of the discharge in the 1<sup>st</sup> ionization stage of the two-stage TAL. In particular, the ionization processes are studied in detail in the model of the 1<sup>st</sup> stage. The following input parameters are used to set up the problem: mass flow rate, discharge voltage, thruster geometry and magnetic field distribution. Electron temperature calculated in the acceleration stage is used as a boundary condition. In the case of a 3kV acceleration stage voltage, the electron temperature at the interface between the two stages is about 18.5 eV. It is interesting to note that the electron temperature increases with voltage decrease in the acceleration stage due to increase of the electron flux to the wall across the sheath and associated losses. In the ionization stage, the energy equation (Eq.5) is simplified and simple linear dependence of the electron

temperature on the discharge voltage is used:  $T_e = \beta U_d$ . According to previous models of the anode layer, it can be assumed that  $\beta=0.1$  (Ref. 18). Thus a higher discharge voltage will lead to a higher electron temperature in the ionization region.

The ionization fraction distribution in the ionization layer is shown in Fig. 2 with discharge voltage as a parameter. Higher discharge voltage leads to higher electron temperature that in turn affects the ionization rate. As a result, one can see that the higher discharge voltage causes a higher ionization degree near the anode. The ionization fraction sharply increases near the anode at a distance of about millimeter and then saturates at the level dependent on the discharge voltage.

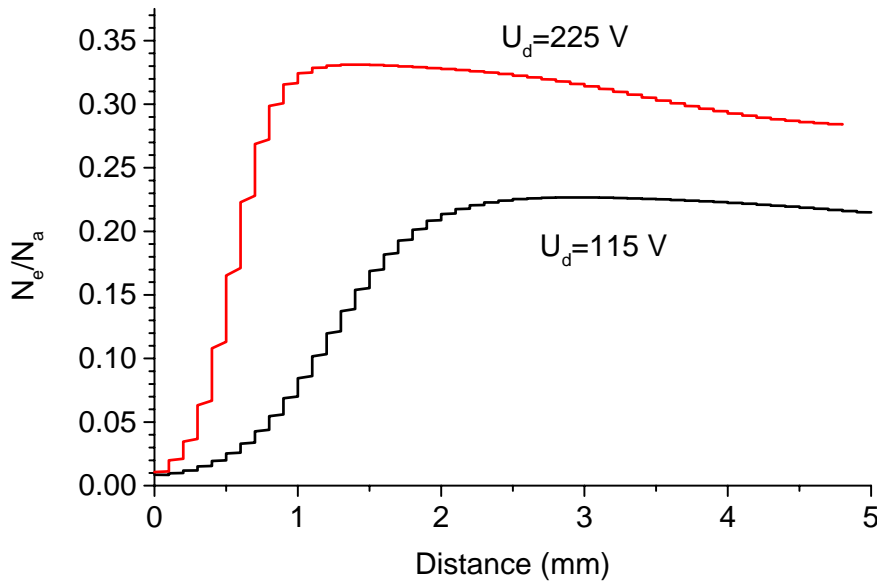


**Fig.2. Ionization fraction in the ionization layer near the anode with discharge voltage as a parameter.**

The two-dimensional density distribution in the first stage is shown in Fig.3. It can be seen that the plasma density peaks near the anode due to strong ionization and then decreases due to acceleration of the ions along the channel.

One of the most important parameters of the discharge is the current-voltage characteristic. The calculated characteristic for the 1<sup>st</sup> stage is shown in Fig.4. According to model prediction, the discharge current increases with the discharge voltage. Higher discharge current is supported by increased ionization as shown above. The typical experimental characteristic is also shown in Fig.4. It can be seen that the thruster has an optimal discharge characteristic in a narrow range of discharge voltage. This optimal range of the discharge voltage is calculated here. Higher discharge voltage (above 250 V) leads to very high electron temperature in the 1<sup>st</sup> stage and causes significant increase of the discharge current as well as the acceleration stage current. The discharge current in the 1<sup>st</sup>

stage increases with the voltage, while the discharge current in the second stage is fairly constant. The discharge current increases due to ionization increase in the vicinity of the anode as shown in Fig. 2. On the other hand, the plasma density at the exit of the 1<sup>st</sup> stage is fairly independent of the discharge voltage thus leading to flat dependence of the acceleration stage current on the discharge voltage. One can see that our model predictions are in good agreement with experiment.

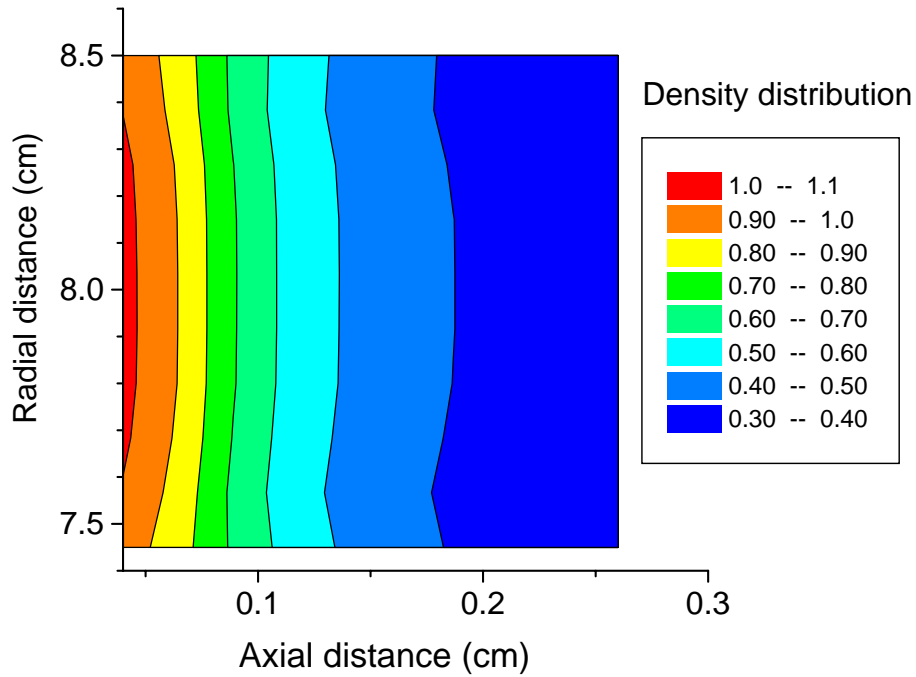


**Fig. 3. Density distribution in the 1<sup>st</sup> stage.**

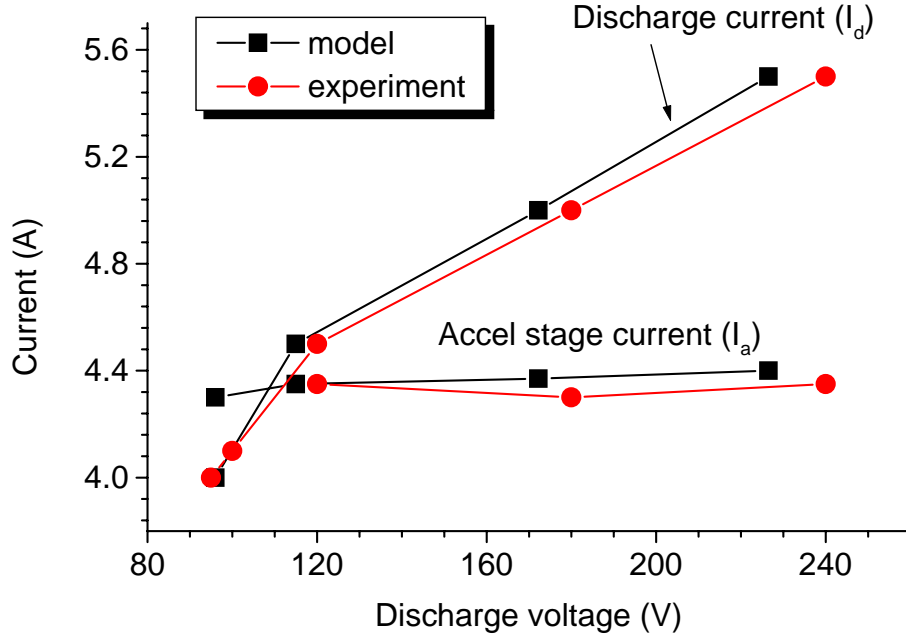


**Fig. 4. Current-voltage characteristics of the 1<sup>st</sup> stage and dependence of the acceleration stage current on the discharge voltage in the 1<sup>st</sup> stage. Comparison with experimental data. Experimental data were taken from Ref. 14.**

#### IV. Analysis of the acceleration stage

The solution of the plasma flow in the 1<sup>st</sup> stage provides the boundary conditions for the acceleration stage. In the acceleration stage, a coupled problem of the quasi-neutral plasma region and the near-wall sheath is considered. Our previously developed model of the acceleration stage [15] is extended to include the effect of sheath expansion. It was shown that the length of the acceleration channel cross section decreases due to sheath expansion [15]. This effect can be explained by invoking the following simple argument. When a negative voltage (cathode potential in the case considered) is applied to a surface immersed in a plasma, electrons are repelled from the surface, leading to sheath formation. Electrons drift away from the surface due to the presence of the high electric field. In the steady state, the ions are then accelerated toward the surface by the electric field of the sheath. In the one-dimensional steady state case the sheath thickness can be estimated according to the Child-Langmuir law:<sup>19,20</sup>

$$s = \left(\frac{4}{9}\epsilon\right)^{1/2} \left(\frac{2e}{m_i}\right)^{1/4} \frac{U^{3/4}}{(eZ_i N_s V_s)^{1/2}} \quad (7)$$

In a bismuth TAL, the channel wall has a potential equal to the cathode potential and therefore the voltage across the sheath,  $U$ , is equal to the plasma potential and varies along the channel. Similarly, the steady state sheath thickness in a partially magnetized plasma was calculated in a plasma immersion ion implantation system.<sup>21</sup> One can see that

the steady-state sheath thickness is determined by the plasma density and ion velocity at the sheath edge for a given bias voltage. In general, the high voltage sheath expands significantly and the quasi-neutral plasma region is confined in the middle of the channel. For instance, in the case of a 5 kV discharge voltage, the sheath thickness is about several centimeters, which is a significant portion of the channel width. Thus, sheath expansion leads to a decrease of the acceleration region length.

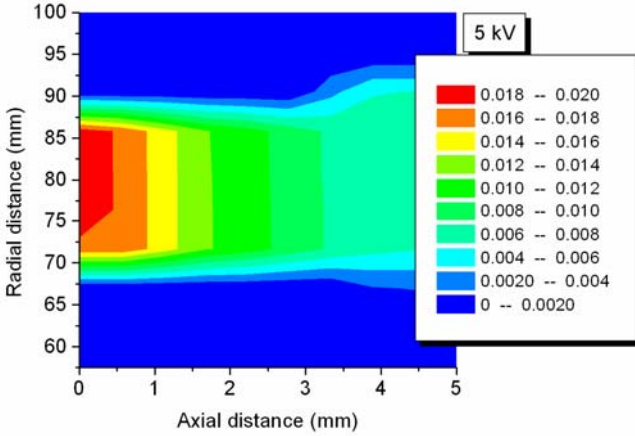


**Fig. 5. Electron density distribution in the acceleration channel. The wall has the cathode potential. Electrons are depleted from the sheath due to large potential drop.**

The typical plasma density distribution in the acceleration channel is shown in Fig.5. In these calculations, electron depletion due to the high-voltage sheath expansion is taken into account. The plasma-sheath interface is considered as a boundary for the quasi-neutral plasma flow. One can see that the quasi-neutral plasma region is confined in the middle of the channel especially at the anode side of the channel.

One of the important parameters of the acceleration region is the acceleration layer length. Previously, it was shown that the acceleration layer length decreases due to effect of the sheath near the wall.<sup>15</sup> This effect can be explained using rather simple physical reasoning. The acceleration layer length is determined by the balance between the electron flux and electron drift across the magnetic field:

$$e\mu_{\perp}n_eE = j_e = \frac{I}{A(s)} \quad (8)$$

where  $A(s)$  is the acceleration channel cross section dependent on the sheath thickness,  $s$ . The electric field can be estimated as  $U_a/d_a$ , where  $d_a$  is the acceleration layer length. Taking this into account and assuming the Bohm-type electron mobility across the magnetic field  $\mu_{\perp}=I/(\alpha B)$  one can obtain:

$$d_a \sim r_{ce}A(s) \quad (9)$$

Thus, one can see that the acceleration layer length decreases with  $A(s)$  decrease due to sheath expansion.

## V. Erosion study

Based on the output from the model, we calculated the erosion of the guard ring which is the most critical part of the 2<sup>nd</sup> stage of the considered TAL. Unfortunately, there are no available data on sputtering coefficients for many materials under bismuth bombardment. Based on the fact that sputtering data for mercury is available and that these data are very close to the data for bismuth we use mercury sputtering coefficients in our calculations.<sup>22,23</sup> We consider guard ring walls made out of molybdenum in order to compare model predictions with some available experimental data summarized in Ref.14. The sputtering yield depends on the ion energy and angle of incidence. Due to sheath expansion in the acceleration stage as considered in the previous section, ions accelerate to the wall across the sheath to the energy equivalent of the sheath potential drop. This adds to the ion energy due to acceleration in the electric field in the axial direction. Towards the exit plane, the potential drop across the sheath decreases thus the ion velocity component normal to the wall also decreases. The sheath thickness distribution along the acceleration channel and dependence on the acceleration voltage are shown in Fig.6. It can be seen that the sheath thickness significantly decreases towards the thruster exit plane. This effect will be important in the evaluation of the erosion profile as will be described below.

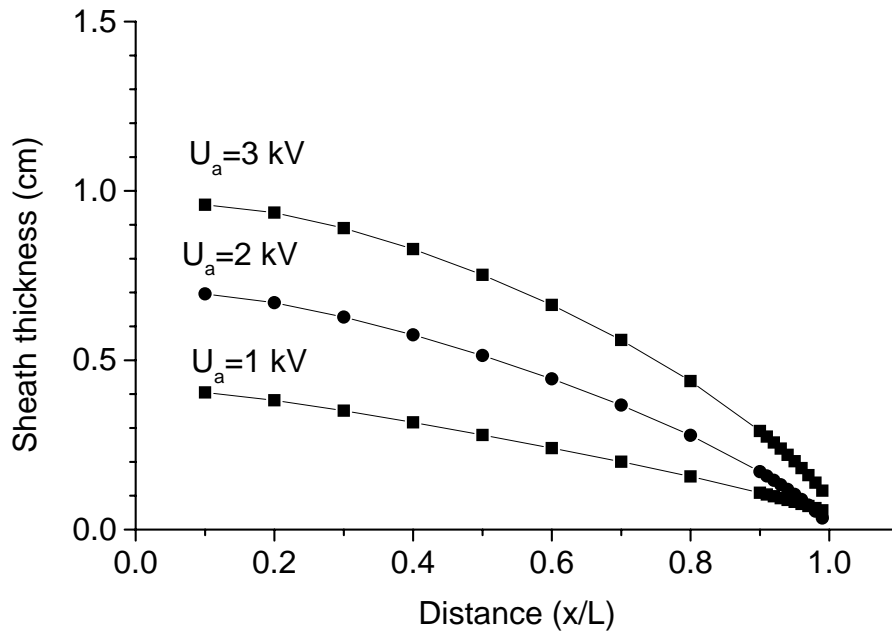


Fig. 6. Sheath thickness with acceleration voltage as a parameter.

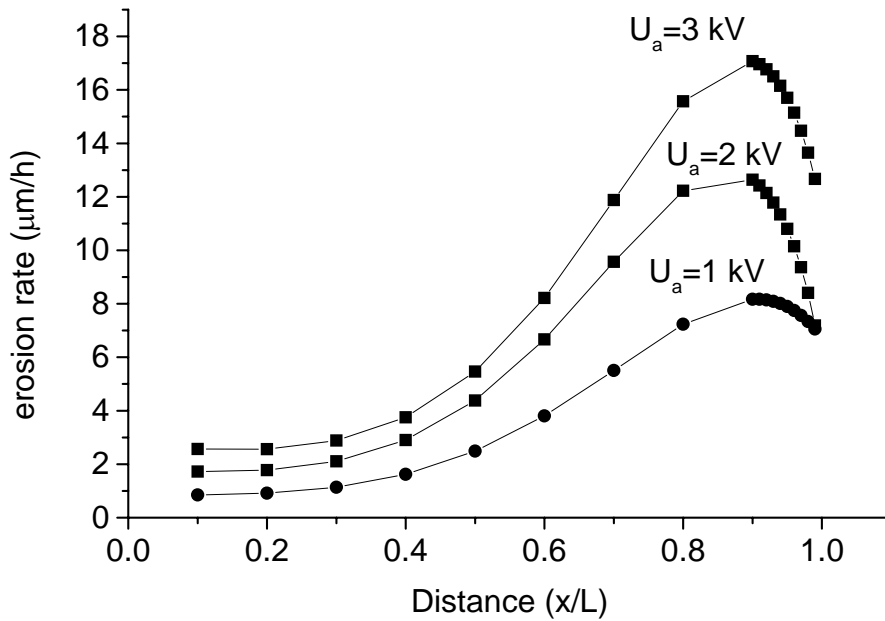


Fig. 7. Erosion rate distribution with the acceleration voltage as a parameter. Mass flow rate=10 mg/s,  $I_a=5$  A.

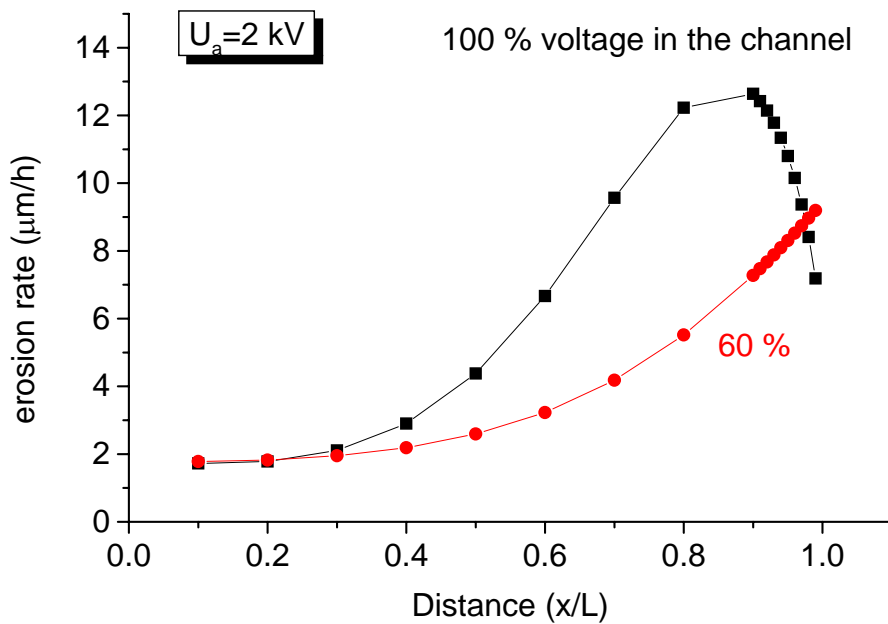


Fig. 8. Erosion rate distribution with the voltage drop inside the acceleration channel as a parameter. Mass flow rate=10 mg/s,  $I_a=5$  A,  $U_a=2$  kV.

The calculated erosion rates with acceleration voltage are shown in Fig.7. One can see that erosion peaks inside the channel near the exit plane. The erosion rate then decreases towards the exit plane due to decrease of the potential drop in the radial direction in the sheath. On the other hand, the erosion rate profile depends on the fraction of the voltage inside the channel as shown in Fig. 8. In the case of entire voltage drop inside the channel, the erosion rate peaks near the exit plane, while in the case of significant voltage fraction in the near plume, the erosion profile has its peak at the exit plane. The later dependence is more consistent with the experimental observations<sup>14</sup>. It is known that in general significant ion acceleration occurs in the near plume, thus suggesting that one should consider only a fraction of the acceleration voltage inside the channel. It should be pointed out that the overall erosion profile and the total erosion of the guard ring wall are consistent with experimental observations<sup>14</sup>.

## VI. Plume study

Plume modeling is also being conducted for spacecraft integration assessment. Some preliminary results are presented here. The number density at the exit of the thruster is of the order of  $10^{16}$ - $10^{18}$   $m^{-3}$ . This indicates that the flow is not in the hydrodynamic regime, but also that there will be some collisions that need to be taken into account. The numerical approach employed in the present work employs a hybrid particle-fluid approach. The bismuth ions (only singly charged) and atoms are simulated as particles using the direct simulation Monte Carlo (DSMC) method<sup>24</sup> to simulate collisions, and the Particle-In-Cell (PIC) method<sup>25</sup> to accelerate the ions self-consistently in electrostatic fields. Due to their significantly smaller length and time scales, electrons are simulated using a hydrodynamic fluid approach. In the present work, the electron fluid model simply uses the Boltzmann relation that provides the plasma potential based on the plasma number density that is obtained directly from the spatial distribution of the ions under the assumption of charge neutrality. While more advanced electron fluid models have been developed recently for xenon plasma plumes,<sup>26</sup> the Boltzmann relation is considered a sufficient approach for this preliminary study. A critical aspect of these simulations concerns the cross sections for charge and momentum exchange as these are important mechanisms leading to plume divergence. In the present work, the charge exchange cross sections employ the semi-empirical general model of Sakabe and Isawa.<sup>27</sup> When a charge exchange event occurs between a bismuth ion and a bismuth atom, it is assumed that no collisional scattering occurs. Based on conclusions drawn for a xenon plasma,<sup>28</sup> it is assumed that the momentum exchange cross section between an ion and an atom is identical to that for charge exchange. For momentum exchange between two atoms, the Variable Hard Sphere (VHS) collision model of Bird<sup>24</sup> is employed. Coulomb collisions are omitted from the present analysis. All momentum exchange collisions are assumed to follow isotropic scattering.

Most of the properties at the thruster exit are obtained from the thruster modeling. The ion temperatures are varied in order to obtain the best agreement with the available experimental data. The plasma potential in the thruster exit is assumed to be 0 V and the electron temperature in the Boltzmann model is 15 eV. In Figs. 9a and 9b, contours of the ion and atom number densities are shown, respectively. The simulations are conducted at a finite back pressure of  $10^{-5}$  torr. These results clearly indicate the very focused beam that is produced by the VHITAL

thruster. Indications of charge exchange ions escaping from the main beam are also present. Very limited experimental data in the plume is available from the Russian experiments of the 1980's. The most reliable data consists of radial profiles of ion current density taken 70 cm downstream of the thruster exit. Figure 10 shows a comparison between these measured data and the simulation data obtained with a thruster exit ion temperature of 1 eV. The simulation results offer good agreement with the measured data, but are sensitive to the values assumed at the thruster exit plane for the ion temperature. Future plume simulation work will consider additional experimental data sets as well as working towards the inclusion of magnetic field effects on the plume plasma.

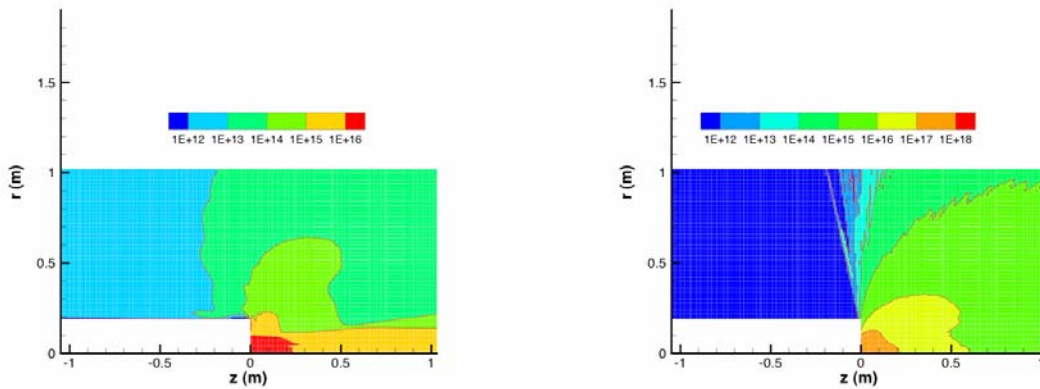


**Figure 9. Number density ( $m^{-3}$ ) contours in the VHITAL plume for (a) ions and (b) atoms.**

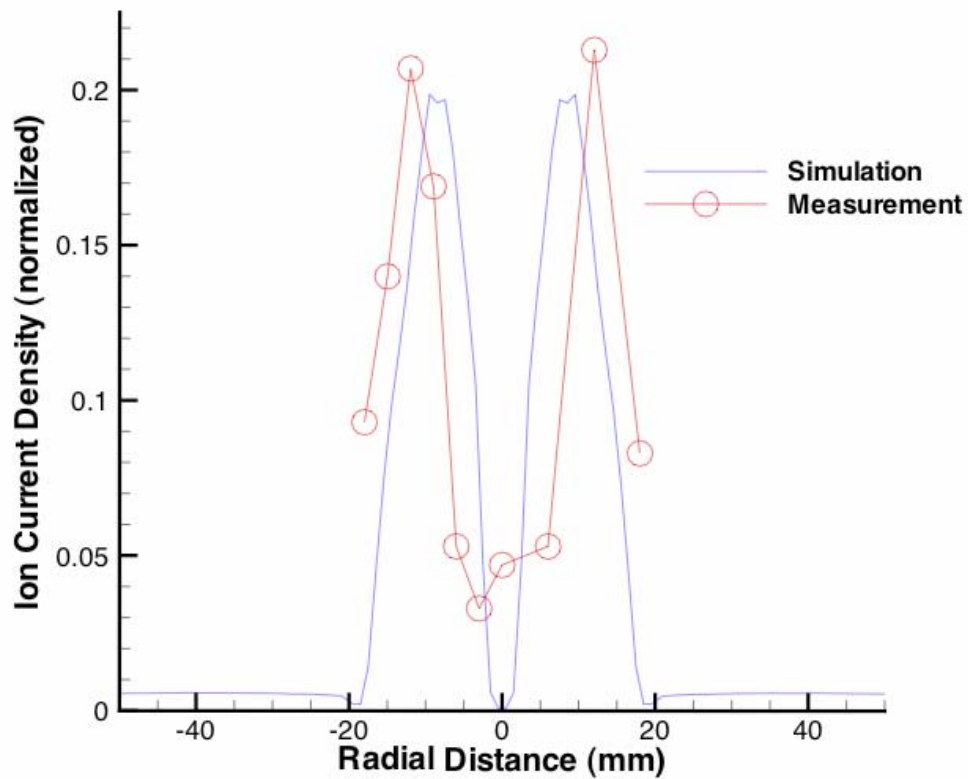


Figure 10. Radial profile of ion current density at 70 cm from the thruster exit.

## VII. Concluding remarks

In this paper, a model of a two-stage thruster with anode layer based on a two-dimensional hydrodynamic approach was described. We considered both ionization and acceleration stages separately, having used the solution of the 1<sup>st</sup> stage as the boundary conditions for the 2<sup>nd</sup> stage. It was found that the predicted current-voltage characteristic of the discharge in the 1<sup>st</sup> stage is in a good agreement with experiment. The thruster has an optimal discharge characteristic in terms of fairly constant acceleration current in a narrow range of discharge voltage (90-250 V). Higher discharge voltage (above 250 V) leads to very high electron temperature in the 1<sup>st</sup> stage and causes significant increase of the discharge current as well as the acceleration stage current. In the acceleration channel, plasma –wall interactions such as formation of the near wall sheath was considered. An expansion of the high

voltage sheath near the acceleration channel wall was investigated. The model predicted that under the typical conditions, the near-wall sheath expands significantly and the quasi-neutral plasma region is confined in the middle of the channel. For instance, in the case of a 3 kV discharge voltage, the sheath thickness is about 1 cm, which is a significant portion of the channel width. In addition it was shown that near-wall sheath expansion leads to shorter acceleration region.

Based on the plasma properties in the acceleration region, the guard ring erosion profile was calculated and it was shown that the erosion rate profile depends on the fraction of the voltage inside the channel. In the case of entire voltage drop inside the channel, the erosion rate peaks near the exit plane, while in the case of significant voltage fraction in the near plume, the erosion profile has its peak at the exit plane. The erosion profile and the total erosion of the guard ring wall were found to be consistent with experimental observations.

Plasma flow analysis provided the boundary conditions for the plume expansion study. A hybrid particle-fluid model of the thruster plume was developed. It was shown that the ion current density distribution in the plume generally agrees well with available experimental data thus partially validating our overall modeling approach.

### **Acknowledgment**

The research was funded by NASA's Exploration Systems Missions Directorate, managed by John Warren, Associate Director for Advanced Systems and Technology, Prometheus Nuclear Systems and Technology Program.

---

## References

- <sup>1</sup> “Physics and application of plasma accelerators”, Ed. A.I. Morozov, Minsk, 1974 (in Russian)
- <sup>2</sup> G. Seikel and E. Reshotko, *Bull. Am. Phys. Soc.* 7, 414 (1962).
- <sup>3</sup> F. Salz, R.G. Meyerand and F. Salz, *Bull. Am. Phys. Soc.*, 7, 441 (1962)
- <sup>4</sup> R.J. Etherington and M.G. Haines, *Phys. Rev. Lett.*, **14**, 1019 (1965)
- <sup>5</sup> G.S. Janes and R.S. Lowder, *Phys. Fluids*, **9**, 1115 (1966)
- <sup>6</sup> A.V. Zharinov and Yu.S. Popov, *Sov. Phys. Tech. Phys.*, **12**, 208 (1967)
- <sup>7</sup> A.I. Morozov, *Sov. Phys. Dokl.*, **10**, 775 (1966)
- <sup>8</sup> V.V. Zhurin, H.R. Kaufman and R.S. Robinson, *Plasma Sources Sci. Technol.*, **8**, 1 (1999)
- <sup>9</sup> A.I. Morozov and V.V. Saveliev, in *Review of Plasma Physics*, Ed. By B.B. Kadomtsev and V.D. Shafranov (Consultant Bureau, New York, 2000), Vol. 21, p. 203.
- <sup>10</sup> D.T. Jacobson, R.S. Jankovsky, V.K. Rawlin, D.H. Manzella, 37<sup>th</sup> AIAA Joint Propulsion Conference, Salt Lake City, UT, 2001, (American Institute of Aeronautics and Astronautics, Washington DC, 2001), AIAA-2001-3777
- <sup>11</sup> S. Tverdokhlebov, A. Semenkin, and J. Polk, 40<sup>th</sup> AIAA Aerospace Sciences Meeting, Reno, NV, 2002, (American Institute of Aeronautics and Astronautics, Washington DC, 2002), AIAA Paper 2002-0348
- <sup>12</sup> C. Marrese-Reading et al., The VHITAL program to demonstrate the performance and lifetime of a bismuth-fueled very high Isp Hall thruster, AIAA-2005-4564.
- <sup>13</sup> A.E. Soloduchin and A.V. Semenkin, 28<sup>th</sup> Inter. Conference on Electric Propulsion, Toulouse, France, (The Electric Rocket Propulsion Society, Worthington, OH, 2003), IEPC-2003-0204
- <sup>14</sup> V.E. Erofeev and L.V. Leskov, Hall accelerator with anode layer, In book “Physics and application of plasma accelerators”, Ed. A.I. Morozov, Minsk, 1974, pp. 18-47 (in Russian)
- <sup>15</sup> M. Keidar, I.D. Boyd and I.I. Beilis, Modeling of a high-power thruster with anode layer, *Physics of Plasmas*, 11, No. 4, 2004, pp. 1715-1722.
- <sup>16</sup> M. Keidar, I.D. Boyd and I.I. Beilis, Plasma flow and plasma-wall transition in Hall thruster channel, *Physics of Plasmas*, 8, No. 12, 2001, pp. 5315-5322.
- <sup>17</sup> R.S. Freund, R.C. Wetzel, R.J. Shul, and T.R. Hayes, Cross-section measurements for electron-impact ionization of atoms, *Phys. Rev. A*, Vol. 41, No. 7, 1990, pp. 3575-3595.
- <sup>18</sup> Yu.S. Popov, Penning low-pressure discharge with cold cathode, *Sov. Phys. Tech. Phys.*, vol. 37, No. 1, 1967, pp. 118-126.
- <sup>19</sup> C. D. Child, *Phys. Rev.*, **32** 492 (1911)
- <sup>20</sup> I. Langmuir, *Phys. Rev.*, Ser. II 2 450 (1913)
- <sup>21</sup> M. Keidar, O.R. Monteiro, A. Anders, I.D. Boyd. *App. Phys. Lett.*, **81** (7) 1183 (2002)
- <sup>22</sup> N.V. Pleshivtzev, “Cathode sputtering”, Atomizdat, Moscow, 1986 (in Russian)
- <sup>23</sup> Fundamental and applied aspects of solid material sputtering, Ed. E.S. Mashkova, 1989, Mir, Moscow (in Russian)
- <sup>24</sup> Bird, G.A., *Molecular Gas Dynamics and the Direct Simulation of Gas Flows*, Oxford University Press, Oxford, 1994.
- <sup>25</sup> Birdsall, G.A. and Langdon, B, *Plasma Physics Via particle Simulation*, Adam Hilger Press, Oxford, 1994.
- <sup>26</sup> Boyd, I.D. and Yim, J.T., “Modeling of the Near-Field Plume of a Hall Thruster,” *Journal of Applied Physics*, Vol. 95, 2004, pp. 4575-4584.
- <sup>27</sup> Sakabe, A. and Izawa, Y., “Simple Formula for the Cross Sections of Resonant Charge Transfer Between Atoms and Their Positive Ions at Low Impact Velocity,” *Physical Review A*, Vol. 45, 1992, pp. 2086-2089.
- <sup>28</sup> Boyd, I.D. and Dressler, R.A., “Far-field Modeling of the Plasma Plume of a Hall Thruster,” *Journal of Applied Physics*, Vol. 92, 2002, pp. 1764-1774.